Tellus (2003), 55B, 522–529
Printed in UK. All rights reserved

TELLUS
ISSN 0280–6509

Effect of recent observations on Asian CO_2 flux estimates by transport model inversions

By SHAMIL MAKSYUTOV[1,2]*, TOSHINOBU MACHIDA[2], HITOSHI MUKAI[2], PRABIR K. PATRA[1], TAKAKIYO NAKAZAWA[3,1], GEN INOUE[3] and TRANSCOM-3 MODELERS[4], [1]*Frontier Research System for Global Change, 3173-25 Showa-machi, Kanazawa-ku, Yokohama, 236-0001, Japan;* [2]*National Institute for Environmental Studies, Tsukuba, 305-8506, Japan;* [3]*Center for Atmospheric and Oceanic Studies, Tohoku University, Sendai, 980-8578, Japan;* [4]*D. Baker, P. Bousquet, L. Bruhwiler, Y-H. Chen, P. Ciais, A. S. Denning, S. Fan, I. Y. Fung, E. Gloor, K. R. Gurney, M. Heimann, K. Higuchi, J. John, R. M. Law, T. Maki, P. Peylin, M. Prather, B. Pak, P. J. Rayner, S. Taguchi, T. Takahashi, C-W. Yuen*

(Manuscript received 2 January 2002; in final form 3 December 2002)

ABSTRACT

We use an inverse model to evaluate the effects of the recent CO_2 observations over Asia on estimates of regional CO_2 sources and sinks. Global CO_2 flux distribution is evaluated using several atmospheric transport models, atmospheric CO_2 observations and a "time-independent" inversion procedure adopted in the basic synthesis inversion by the Transcom-3 inverse model intercomparison project. In our analysis we include airborne and tower observations in Siberia, continuous monitoring and airborne observations over Japan, and airborne monitoring on regular flights on Tokyo–Sydney route. The inclusion of the new data reduces the uncertainty of the estimated regional CO_2 fluxes for Boreal Asia (Siberia), Temperate Asia and South-East Asia. The largest effect is observed for the emission/sink estimate for the Boreal Asia region, where introducing the observations in Siberia reduces the source uncertainty by almost half. It also produces an uncertainty reduction for Boreal North America. Addition of the Siberian airborne observations leads to projecting extra sinks in Boreal Asia of 0.2 Pg C yr^{-1}, and a smaller change for Europe. The Tokyo–Sydney observations reduce and constrain the Southeast Asian source.

1. Introduction

Inverse models of global carbon dynamics use models of atmospheric transport to retrieve terrestrial and oceanic carbon fluxes from the observations of spatial and temporal distributions of the atmospheric carbon dioxide concentration. These estimates of the annual average flux of carbon usually indicate that the northern hemispheric land is a carbon sink (e.g. Tans et al., 1990). However, the attempts to use spatial structure of the observed concentrations to deduce the annual average fluxes for large terrestrial and oceanic regions resulted in large spread in the estimations for regions residing in the same latitude bands such as North America and Eurasia (Fan et al., 1998; Rayner et al., 1999; Bousquet et al., 2000).

The reasons for the differences between inverse model results are believed to originate in model transport (Law et al., 1996; Gurney et al., 2002) and inverse modeling approaches. Another factor limiting the application of the inverse modeling to discriminate the carbon fluxes between land regions is lack of the observations close to the target areas. One of the main reasons to avoid the continental locations in designing the observing network in the past was the large variability of the surface carbon dioxide concentration near the sources. Problems come from large temporal and spatial variability in terrestrial carbon dioxide fluxes, and the rate of surface layer mixing, which are being

*Corresponding author.
e-mail: shamil@jamstec.go.jp

addressed during the recent decade by sampling the air at higher elevations using tall towers (Bakwin et al., 1995) and aircraft (e.g. Nakazawa et al., 1993).

In this paper, we evaluate recent improvements in the observational coverage of the Asian continent and Asian outflow areas. We combine the surface and airborne observations over Siberia, Japan and tropical South-East Asia with the transport model inversion analysis by Gurney et al. (2002). By using several transport models in the analysis we aim at reducing uncertainties in the estimated carbon dioxide flux distribution with inclusion in the additional observations. We attempt to identify discrepancies between models and observations that may lead to improvements in models, observations and data analysis.

2. Material and methods

We follow the basic inverse model analysis by Transcom-3 project (Gurney et al., 2002) as the base for our analysis, so we can use the Transcom-3 basic inversion as a reference and omit describing some details in this paper. The difference between the Transcom-3 inversion and our procedure is limited to using fewer models, preparation of the atmospheric data for additional sites, and, in the case of additional data, the time periods for which the annual averages are calculated.

2.1. *Inverse model analysis*

Basic "time-independent" inverse model analysis by the Transcom-3 project uses a Bayesian synthesis inversion to derive the estimates for surface fluxes of carbon dioxide using the annual average concentration of carbon dioxide as reported by the Globalview CO_2 data integration project (Globalview, 2000). The Bayesian inverse modeling procedure is described in detail elsewhere (Enting et al., 1995), and numerical realization of the algorithm is based on one described in Rayner et al. (1999).

In Bayesian synthesis inversion (Tarantola, 1987), a cost function (F) is minimized to reduce the mismatches between the atmospheric observations D^0 and transport model predicted responses to surface fluxes $D = \boldsymbol{G} \cdot S$ (matrix $\boldsymbol{G}$ represents a transport operator), and a priori sources S^0 and predicted sources S:

$$F = (\boldsymbol{G} \cdot S - D^0) \cdot C_D^{-1} \cdot (G \cdot S - D^0)^T + (S - S^0) \cdot C_S^{-1} \cdot (S - S^0)^T$$

The misfits between predicted and a priori parameters are weighted by error covariance matrices C_D for concentrations and C_S for regional sources. We assume those matrices are diagonal with diagonal elements equal to squared uncertainties of CO_2 concentrations and sources. The transport models calculated the annual average atmospheric CO_2 responses to the fluxes from fossil fuel combustion (Andres et al., 1996), the terrestrial biosphere by the CASA model (Randerson et al., 1997) and ocean–atmosphere exchange (Takahashi et al., 1999), provided as seasonally varying global fields. In addition, the annual average responses to the fluxes from 22 large regions (11 land and 11 oceanic regions) are prepared in order to model the effects of the regional sources and sinks (Gurney et al., 2000). Regions are listed later in the paper (see Table 3). The inverse model solution provides optimal estimates for regional fluxes that minimize the cost function F. It also provides a mathematical expectation for statistical error of the flux estimate, which we call the flux uncertainty. The expression for the flux uncertainty was derived by Tarantola (1987) as follows:

$$\tilde{C}_S = \left(G^T \cdot C_D^{-1} \cdot G + C_S^{-1}\right)^{-1}.$$

In practice, a pseudo-inverse of the matrix $G^T \cdot C_D^{-1} \cdot G + C_S^{-1}$ is evaluated by standard singular value decomposition procedure; see Rayner et al. (1999) for details.

Unlike the analysis by Gurney et al. (2002) that uses 16 transport models, we use an earlier subset of 14 transport model outputs. The transport models used in the study are: GISS-UCB, UCI-CTM (three model variants), JMA-CDTM, MATCH-CCM3 winds, MATCH-NCEP winds, MATCH-CRC version, NIES, NIRE, RPN, SKYHI, TM2, TM3. A difference in mean flux results between our basic inversion and one by Gurney et al. (2002, 2003) is minor as compared to flux uncertainty estimates. Inversion was performed with the basic observational dataset (Globalview, 2000) and the extended one (described in Section 2.2). For data uncertainty a basic procedure adopted values determined as a root-mean square average of the difference between Globalview fits and actual observed concentrations. The lower threshold for data uncertainty in our analysis was set to 0.3 ppm, instead of 0.25 ppm as in (Gurney et al., 2002). The transport model predicted monthly average three-dimensional fields were interpolated vertically to the site pressure level. Instead of horizontal interpolation, the model simulated concentration was chosen from a grid cell with center closest to the site location.

Table 1. *Asian observation sites and data included into the analysis*

Site	Year	Altitude	Analysis	Reference
Surgut, 61°N, 73°E	93–98	0.5–7 km	Flasks	Machida et al. (2000)
Yakutsk, 62°N, 130°E	96–98	1–5 km	Flasks	”
Novosibirsk, 55°N, 83°E	97–98	0.5–7 km	Flasks	”
Hateruma, 24°N, 123°E	94–98	10 m ASL	NDIR	Mukai et al. (2000a)
Cape Ohchi-ishi, 43°N, 145°E	96–98	49 m ASL	NDIR	Mukai et al. (2000b)
Sendai, 37°N, 140°E	92–98	0.5–9 km	Flasks	Nakazawa et al. (1993)
Tokyo–Sydney 30°N–30°E	93–96	10–12 km	Flasks	Matsueda et al. (2002)

2.2. *Observations and data processing*

In addition to using the Globalview (2000) data for 1992–1996 as in Gurney et al. (2002), we include airborne observations in West and Central Siberia (Machida et al., 2000), continuous monitoring (Mukai et al., 2000a,b) and airborne observations in Japan (Nakazawa et al., 1993), and the airborne monitoring on regular flights on Tokyo–Sydney route (Matsueda et al., 2002). Table 1 gives information on the additional observation sites. The data of the airborne sampling for 1992–1996 over Japan were not published elsewhere and are based on the results of the recent measurements. The observation procedures and quality control are same as reported by Nakazawa et al. (1993).

Following the basic Transcom inversion procedure, we select Globalview sites that have more than 70% of data available during 1992–1996 (total of 78 selected). The time period we use for our additional data (1992–1998) does not exactly match with that of the basic Transcom-3 procedure (Globalview data, 1992–1996). We select wider time frame for additional data in order to compensate for effects of significant day-to-day variability on the low-frequency aircraft sampling (Machida et al., 2000), which is conducted once a month. We assume that extending the averaging period reduces the effect of the inter-annual variability in observed annual average concentration difference vs. South Pole data. The possible differences in fossil-fuel and biogenic-emission signals between these two periods are ignored as well as an inter-annual variability in transport. The effects of interannual variability in the annual average concentration data on CO_2 inversion by Transcom procedure are studied by Law et al. (2003).

To prepare multiyear average concentration data for each additional site we first derive the CO_2 trend at South Pole from monthly CMDL flask data for 1991–1998 (downloaded from the CMDL ftp site, 2000), and calculate the average concentration difference with respect to the South Pole trend for each month using all available data for a given site. Then we obtain an annual average concentration from monthly averages. Finally, we add back the South Pole value as defined in the Transcom-3 basic procedure, which is an average of 1992–1996 data by Globalview. This approach considers the CO_2 concentration difference between a particular site and South Pole as single important parameter to determine flux patterns, similar to Fan et al. (1998). Possible inter-calibration errors, that arise from using different reference scales for calibrating the measurements, between additional measurements and those used in Globalview are assumed to be below the observation uncertainties.

The longitudinal plot of the North-hemispheric extratropical observations is presented on Fig. 1. Higher annual average concentration relative to South Pole (above 4 ppm) corresponds to polluted regions in North America, Europe and Asia. Additional observations (not in Globalview 2000) and data uncertainties are summarized in Table 2. Data for the Tokyo–Sidney route are not shown, but are available from WDCGG. The data uncertainties for continuous observations are lower, because we divided the average residual standard deviations (RSDs) by the square root of the number of observations per month. The data uncertainties for low-frequency flask sampling (one flask per month) in this table are representing inter-annual variations of the “monthly” concentration relative to the South Pole trend.

A comparison of the data treatment by the Globalview procedure and our simplified approach was conducted using CMDL observations as an example. In Figs. 2a and 2b we present plots of multi-year average CO_2 concentration relative to South Pole (for the period 1992–1996), and annual average concentration variability, which is used as data uncertainty in the inversion. One can observe that there is a fairly good match in the annual average concentrations

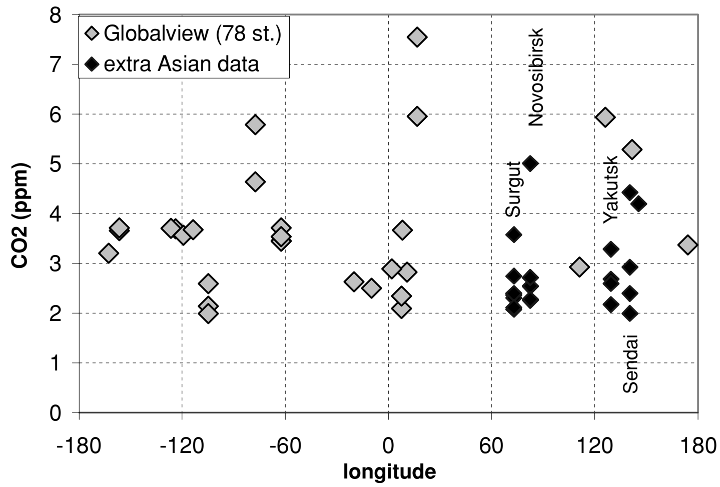

Fig. 1. Extratropical (north of 30°) annual average CO_2 concentrations in the North Hemisphere, relative to South Pole. Additional Asian observations are summarized in Table 2.

between both approaches. Our data treatment procedure makes some overestimation of the data uncertainty when compared to that used in Globalview. The difference indicates that the Globalview fit approaches each particular measurement more closely than the monthly average value estimated with our detrending procedure. Supplying overestimated data uncertainties to inversion is expected to lead to a higher flux uncertainty and an actual underestimation of flux uncertainty reduction due to adding more observations.

In the basic inversion procedure the observed concentration data for collocated sites are combined and data uncertainties adjusted. In the case of the vertical profile measurements, one can think of adjacent vertical levels (such as 500 and 1000 m) as collocated sites, because inside the boundary layer observed concentrations are tightly coupled due to vertical mixing

Table 2. *Multiyear average CO_2 concentrations (relative to South Pole) and its variability*[a]

	Altitude (km)								
Site	Surface	0.5	1	1.5	2	3	4	5.5	7
Surgut		3.58 (0.85)	2.75 (0.74)	2.39 (0.64)	2.37 (0.58)	2.31 (0.57)	2.40 (0.49)	2.08 (0.46)	2.12 (0.47)
Yakutsk			3.29 (0.78)		2.18 (0.48)	2.69 (0.39)	2.60 (0.30)		
Novosibirsk		5.01 (1.09)	2.54 (0.92)	2.26 (0.54)	2.55 (0.46)		2.72 (0.33)		2.72 (0.50)
Hateruma	4.18 (0.20)								
Ohchi-ishi	4.20 (0.20)								
Sendai			4.43 (0.49)			2.93 (0.49)		2.40 (0.23)	2.00 (0.18)

[a]Top number, concentration (ppm); number in parenthesis, concentration data uncertainty, derived from deviations of the individual measurements from the multiyear monthly mean. References to the data are given in Table 1. Sendai data at 1, 3, 5 and 7 km levels combine samples taken over Japan within altitude ranges 0–2, 2–4, 4–6 and 7–8 km. We put 4–6 km average in the 5.5 km column in this table.

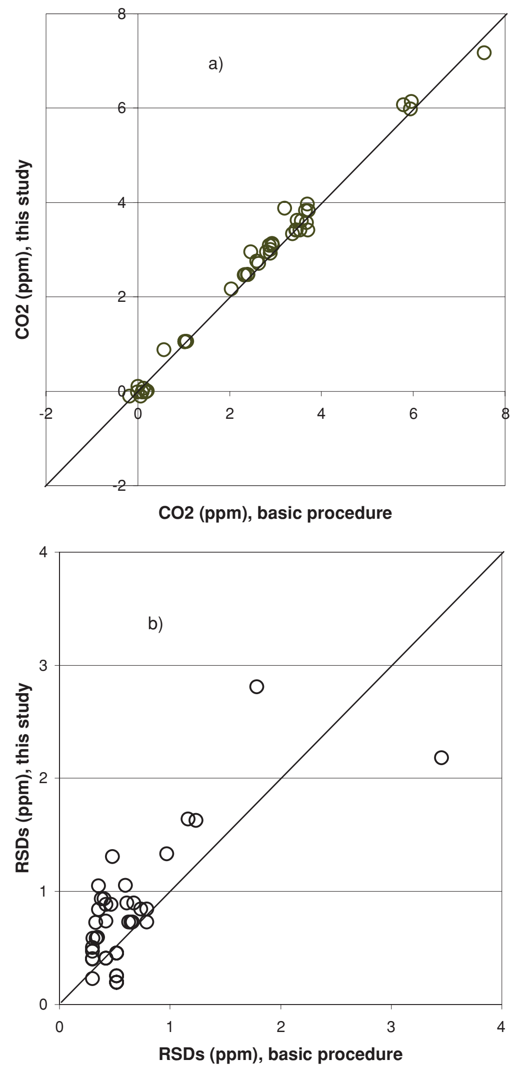

Fig. 2. Comparison of the (a) annual average concentrations (relative to South Pole) and (b) data uncertainties derived from Globalview (as in Transcom-3) and our data treatment procedure.

in summer. However, the vertical coupling disappears in winter, thus we do not consider the effects of coupling, and treat different vertical levels in the same profile as if they are separate sites. According to the inverse problem theory (Tarantola, 1987), a more consistent treatment of the coupled (and correlated) observations should add non-diagonal elements in the observation data error covariance matrix (C_D in the equations above), which is assumed to be diagonal in this study.

3. Results and discussion

The inverse model estimates (average for 14 transport models) for the Asian CO_2 fluxes with and without the additional data are presented in Fig. 3 and Table 3. The inclusion of the data reduces the uncertainty in the estimated regional CO_2 fluxes for Boreal Asia (Siberia), Temperate Asia and South-East Asia. The largest effect is observed for the emission/sink estimate for the Boreal Asia region, where introducing the observations in Siberia reduces the source uncertainty by almost half (from 0.56 to 0.36 Pg C yr^{-1}). It also reduces the uncertainty for Boreal North America, however this happens at the expense of increasing the model-to-model difference for the individual transport model predictions for the region.

The sensitivity of the flux uncertainty estimates to the addition of several combinations of additional sites was tested. In Figs. 4 and 5 we present the relative uncertainty reduction (comparatively to the basic case) and change in the average model-to-model difference (see also Table 3). Annual average CO_2 flux changes are shown in Fig. 6. One interesting result is interdependence of the boreal regions in Asia and North America. Reduction of the flux uncertainty for Siberia is accompanied by a smaller reduction for Boreal North America. As the same time, addition of

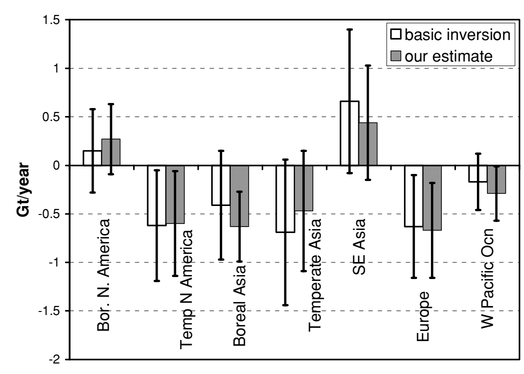

Fig. 3. Model estimates of annual average CO_2 fluxes for Asian regions and related areas. Basic Transcom-3 analysis and our "best" estimate are shown. Error bars indicate inverse model estimates of source uncertainty. Units are Pg C yr^{-1}. Oceanic fluxes are relative to Takahashi et al. (1999) estimates.

Table 3. *Regional CO_2 flux estimates with basic and extended datasets*[a]

Region name	Fluxes		Flux uncertainty		Model spread	
	Basic	Extended	Basic	Extended	Basic	Extended
Boreal N America	0.15	0.27	0.43	0.36	0.27	0.39
Temp N America	−0.62	−0.6	0.57	0.54	0.54	0.56
Trop America	0.59	0.73	1.02	1.0	0.52	0.61
South America	0.01	0.05	0.94	0.93	0.35	0.31
Tropical Africa	−0.36	−0.36	1.0	0.98	0.7	0.81
South Africa	−0.29	−0.1	0.95	0.93	0.39	0.44
Boreal Asia	***−0.41***	***−0.63***	***0.56***	***0.36***	***0.38***	***0.19***
Temperate Asia	***−0.69***	***−0.47***	***0.75***	***0.62***	***0.5***	***0.38***
Tropical (SE) Asia	***0.66***	***0.44***	***0.74***	***0.59***	***0.35***	***0.33***
Australia	0.27	0.27	0.29	0.28	0.19	0.2
Europe	−0.63	−0.67	0.53	0.49	0.34	0.31
North Pacific	0.08	0.1	0.21	0.2	0.16	0.14
West Pacific	−0.17	−0.29	0.29	0.28	0.16	0.21
East Pacific	0.1	0.09	0.28	0.28	0.13	0.15
South Pacific	0.21	0.24	0.45	0.44	0.26	0.26
Northern Ocean	0.12	0.13	0.19	0.19	0.18	0.18
North Atlantic	−0.09	−0.1	0.23	0.23	0.15	0.15
Tropical Atlantic	−0.15	−0.19	0.34	0.33	0.11	0.11
South Atlantic	0.14	0.07	0.47	0.46	0.1	0.12
Southern Ocean	0.43	0.4	0.28	0.28	0.21	0.23
Trop. Indian Ocean	−0.15	−0.15	0.34	0.34	0.14	0.15
South Indian Ocean	0.16	0.15	0.31	0.31	0.13	0.14

[a]Also included are the inverse model estimated flux uncertainties and average model-to-model difference. Units are Pg C yr^{-1}.

the observation sites in Siberia adds to the increased model spread for Boreal North America as well as for other under-constrained regions such as Tropical America. This may be caused by several factors. One possible reason is that Boreal North America is under-constrained by observations. Another factor is that Siberian observations are located in the continental area where model predictions of annual average neutral biosphere signal differ most for different transport models (Gurney et al., 2002), making it yet another difficult area to simulate with transport and biospheric flux models.

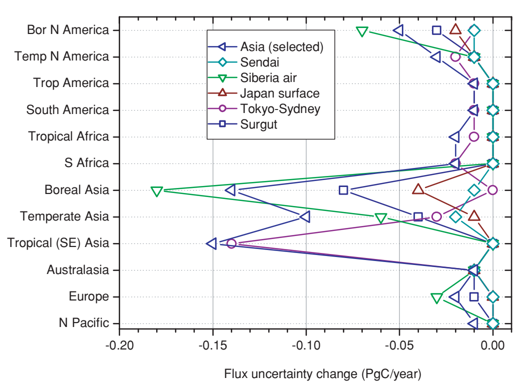

Fig. 4. Change in annual flux uncertainties for all 22 Transcom regions. Site combinations: (1) Asia (selected), all sites except Yakutsk and Novosibirsk profiles (excluded due to short record); (2) Sendai; (3) Siberia air, aircraft profiles over Siberia; (4) Japan surface, Hateruma and Ohchi-ishi; (5) Tokyo–Sydney; (6) Surgut.

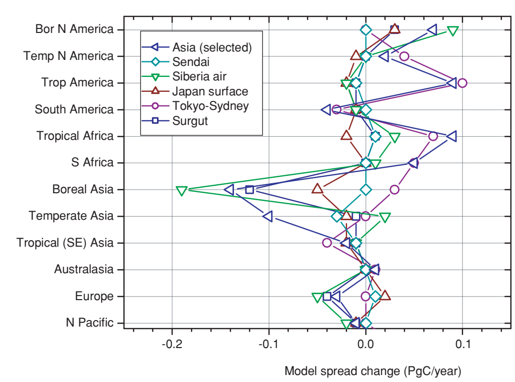

Fig. 5. Change in average model-to-model difference for 22 Transcom regions. Site combinations are the same as in Fig. 4.

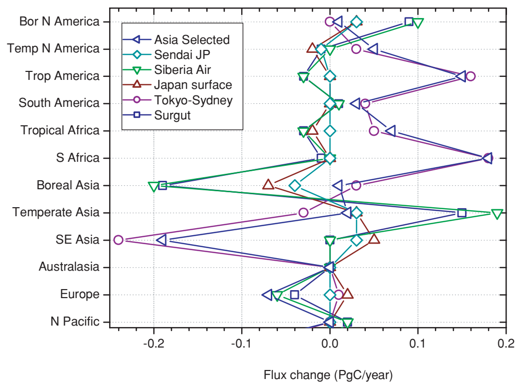

Fig. 6. Change in annual flux for 22 Transcom regions. Site combinations are the same as in Fig. 4.

Inclusion of the Siberian airborne observations leads to extra sinks on Boreal Asia of 0.2 Pg C yr^{-1}, and a smaller change for Europe. We need to take into consideration significant inter-annual variability in the Siberian data (Machida et al., 2000), which we cannot yet explain by the transport and biospheric variations. Inter-annual variability in annual average data can cause large variability in the inverse model flux estimates when using data covering different periods. That could be a reason for differences in estimated effects of Siberian observations between this study and that by Taguchi (2000) that was based on one-year Surgut data. Although the Surgut observations have the longest record, its footprint area represents only a fraction of the Boreal Asia region. In that sense, adding the observations over Novosibirsk and Yakutsk provide a desired improvement in the observational coverage.

Adding the observations over Japan do not produce a major reduction in inversion flux uncertainty for Temperate Asia, because the region's CO_2 flux is already constrained by a number of the observations over China, Korea, Japan and Mongolia included in the Globalview dataset and basic inversion.

The Tokyo–Sydney observations reduce and further constrain the South-East Asian source (Figs. 4 and 6). The result is valuable in the sense that in the area which is not sufficiently covered by surface observations, even the observations remote from the ground (11 km altitude) are still sensitive to surface fluxes and are usable for reducing the inverse model flux uncertainties. This justifies the attempts to use the satellite remote sensing technologies for tropical tropospheric observations, even when those are limited to the upper troposphere. However, proper use of the tropical upper tropospheric observations is also limited by the accuracy of the transport models. The results of the SF_6 transport modeling experiment by Denning et al. (1999) show sizable model-to-model differences in upper tropospheric concentration patterns that are directly translated into the uncertainties of the flux estimations.

4. Summary and conclusions

We use recent CO_2 observations over Asia and the inverse model to improve estimates of the Asian regional CO_2 sources and sinks. The inclusion of the data reduces the uncertainty in the estimated regional CO_2 fluxes for Boreal Asia (Siberia), Temperate Asia and South-East Asia. The largest effect is observed for the emission/sink estimate for the Boreal Asia region, where introducing the observations in Siberia reduces the source uncertainty by about 40%. It also produces a reduction in uncertainty for Boreal North America. Addition of the Siberian airborne observations leads to extra sinks in Boreal Asia of 0.2 Pg C yr^{-1}, and a smaller change for Europe. The Tokyo–Sydney observations tend to reduce and further constrain the South-East Asian source.

We also observed some heterogeneity in the effects of some observations on the Boreal Asia flux estimate, when trying different combinations of sites. It may be useful to try localizing effects of the particular observation sites by using an inversion with a larger number of smaller regions as pointed out by Kaminski et al. (2001).

5. Acknowledgements

This study was made possible through support from Japan's Ministry of the Environment (MOE) and Ministry of Education, Culture, Sports, Science and Technology (MEXT). The Transcom modeling study was supported by the International Geosphere Biosphere Program/Global Analysis, Interpretation and Modeling Project (IGBP/GAIM) and participants' funding agencies. CMDL flask data are provided by the NOAA/CMDL Carbon Cycle Group. S. Fan acknowledges support from NOAA's Office of Global Programs for the Carbon Modeling Consortium.

REFERENCES

Andres, R. J., Marland, G., Fung, I. and Matthews, E. 1996. A 1° × 1° distribution of carbon dioxide emissions from fossil fuel consumption and cement manufacture, 1950–1990. *Global Biogeochem. Cycles* **10**, 419–429.

Bakwin, P., Tans, P., Ussler, W., III and Quesnell, E. 1995. Measurements of carbon dioxide on a very tall tower. *Tellus* **47B**, 535–549.

Bousquet, P., Ciais, P., Peylin, P., Ramonet, M. and Monfray, P. 1999. Inverse modeling of annual atmospheric CO2 sources and sinks 1. Method and control inversion. *J. Geophys. Res*. **104**, D21, 26 161–26 178.

Denning, A. S., Holzer, M., Gurney, K. R., Heimann, M. and coauthors. 1999. Three-dimensional transport and concentration of SF6: A model intercomparison study (TransCom 2). *Tellus* **51B**, 266–297.

Enting, I. G., Trudinger, C. M. and Francey, R. J. 1995. A synthesis inversion of the concentration and δ^{13}C of atmospheric CO_2. *Tellus* **47B**, 35–52.

Fan, S., Gloor, M., Mahlman, J., Pacala, S., Sarmiento, J. and coauthors. 1998. A large terrestrial carbon sink in North America implied by atmospheric and oceanic carbon dioxide data and models. *Science* **208**, 442–445.

GLOBALVIEW-CO_2. 2000. Cooperative Atmospheric Data Integration Project–Carbon Dioxide, 2000. CD-ROM, NOAA CMDL, Boulder, Colorado, U.S.A.

GLOBALVIEW-CO_2. 2001. Cooperative Atmospheric Data Integration Project–Carbon Dioxide, 2001. CD-ROM, NOAA CMDL, Boulder, Colorado, U.S.A.

Gurney, K., Law, R., Rayner, P. and Denning, A. S. 2000. TransCom3 experimental protocol. Paper No. 707, Dept. Atmos. Sci., Colorado State Univ., U.S.A.

Gurney, K., Law, R., Denning, S., Rayner, P. and coauthors. 2002. Towards robust regional estimates of CO_2 sources and sinks using atmospheric transport models. *Nature* **415**, 626–630.

Gurney, K., Law, R., Denning, S., Rayner, P. and coauthors. 2003. Transcom 3 Inversion Intercomparison: Part 1. Annual mean control results and sensitivity to transport and prior flux information. *Tellus* **55B**, in press.

Kaminski, T., Rayner, P., Heimann, M. and Enting, I. 2001. On aggregation errors in atmospheric transport inversions. *J. Geophys. Res.* **106**, 4703–4732.

Law, R., Rayner, P., Denning, A., Erickson, D., Fung, I. and coauthors, 1996. Variations in modeled atmospheric transport of carbon dioxide and the consequences for CO_2 inversions. *Global Biogeochem. Cycles* **10**, 783–796.

Law, R., Chen, Y.-H., Gurney, K. and coauthors. 2003. TransCom3 CO_2 inversion intercomparison: 2. Sensitivity of annual mean results to data choices. *Tellus* **55B**, in press.

Machida, T., Nakazawa, T., Maksyutov, S., Inoue, G. and coauthors. 2000. Variations of atmospheric CO_2 concentrations over Siberia. In: *Proc. 9th Symposium on Joint Siberian Permafrost Studies between Russia and Japan in 1999*. (eds. G. Inoue and A. Takenaka). Isebu, Tsukuba, Japan, 294–299.

Matsueda, M., Inoue, H. and Ishii, M. 2002. Aircraft observation of carbon dioxide at 8–13 km altitude over the western Pacific from 1993 to 1999. *Tellus* **54B**, 1–22.

Mukai, H., Machida, T., Nojiri, Y., Fujinuma, Y. and Katsumoto, M. 2000a. Atmospheric CO_2 monthly mean concentration, Cape Ochi-Ishi. In: *WMO WDCGG Data Report*, JMA, Tokyo, no. 21, 14–15.

Mukai, H., Machida, T., Nojiri, Y., Fujinuma, Y. and Katsumoto, M. 2000b. Atmospheric CO_2 monthly mean concentration, Hateruma. In: *WMO WDCGG Data Report*, JMA, Tokyo, no. 21, 16–17.

Nakazawa, T., Morimoto, S., Aoki, S. and Tanaka, M. 1993. Time and space variations of the carbon isotopic ratio of tropospheric carbon dioxide over Japan. *Tellus* **45B**, 257–274.

Randerson, J., Thompson, M., Conway, T., Fung, I. and Field, C. 1997. The contribution of terrestrial sources and sinks to trends in the seasonal cycle of atmospheric carbon dioxide. *Global Biogeochem. Cycles* **11**, 535–560.

Rayner, P., Enting, I., Francey, R. and Langenfelds, R. 1999. Reconstructing the recent carbon cycle from atmospheric CO_2, δ^{13}C and O_2/N_2 observations. *Tellus* **51B**, 213–232.

Taguchi, S. 2000. Synthesis inversion of the atmospheric CO_2 using NIRE chemical transport model. In: *Inverse Methods in Global Biogeochemical Cycles*. (ed. P. Kasibhatla, M. Heimann, D. Hartley, P. J. Rayner, N. Mahowald and R. Prinn), *Geophys. Monogr. Ser*. **114**, 239–254.

Takahashi, T., Wanninkhof, R. H., Feely, R. A., Weiss, R. F., Chipmann, D. W. and coauthors. 1999. Net sea–air flux over the global ocean: An improved estimate based on the sea-air pCO_2 difference. In: *Proc. 2nd International Symposium on CO_2 in the Oceans*. (ed. Y. Nojiri). CGER-I037-99, CGER/NIES, Tsukuba, Japan, 9–14.

Tans, P., Fung, I. and Takahashi, T. 1990. Observational constraints on the global atmospheric carbon dioxide budget. *Science* **247**, 1431–1438.

Tarantola, A. 1987. *Inverse Problem Theory*, Elsevier, Amsterdam, The Netherlands, 605 pp.